Polymer Journal, Vol. 38, No. 1, pp. 37–43 (2006)

Intrinsic Viscosity of Polyoxyethylene Alkyl Ether C_iE_j Micelles

Satoko SHIRAI, Sachiko YOSHIMURA, and Yoshiyuki EINAGA†

Department of Chemistry, Nara Women's University, Kitauoyanishi-machi, Nara 630-8506, Japan

(Received June 28, 2005; Accepted August 24, 2005; Published January 15, 2006)

ABSTRACT: Micelles of pentaoxyethylene $C_{12}E_5$, hexaoxyethylene $C_{12}E_6$, hepatoxyethylene dodecyl ethers $C_{12}E_7$, and heptaoxyethylene tetradecyl ether $C_{14}E_7$ in dilute aqueous solutions were characterized by viscometry. The intrinsic viscosity $[\eta]$ of the micelles whose size are concentration-dependent were able to be determined at finite concentrations by applying an equation derived by combining the Huggins and Fuoss–Mead equations. The results of $[\eta]$ as a function of the molar mass of the micelle were successfully analyzed by the hydrodynamic theory for wormlike polymers formulated with the touched bead model, indicating that the micelles assume a flexible cylindrical shape. The values of the cross-sectional diameter d have suggested that the surfactant molecules take a randomly coiled form in the micelles. [DOI 10.1295/polymj.38.37]

KEY WORDS Polyoxyethylene Alkyl Ether / Micelle / Intrinsic Viscosity / Wormlike Chain / Wormlike Spherocylinder Model /

Nonionic surfactants polyoxyethylene alkyl ethers $H(CH_2)_i(OCH_2CH_2)_jOH$, abbreviated C_iE_j, form polymerlike micelles in dilute aqueous solution. The micelles grow in size with increasing surfactant concentration and raising temperature, in particular to a great extent when approaching the lower consolute phase boundary. The polymerlike micelles have certain similarities to real polymers and then their solution properties are analogous to those of real polymer solutions. They have been, thus, characterized with the use of experimental techniques employed in the polymer solution studies, such as static (SLS) and dynamic light scattering (DLS),[1–9] small-angle neutron scattering (SANS),[10–12] viscometry,[12,13] pulsed-field gradient NMR,[2–5] and so forth.

However, the micelles possess the essential difference from polymers in the sense that they can break and recombine as sometimes called "living" or "equilibrium" polymers. The micellar size or length is then not chemically fixed but fluctuates around an equilibrium value that, in general, depend on surfactant concentration, temperature, and other factors. This fact means that we have to characterize the micelles under the conditions, especially at finite concentrations, at which the micelles are formed: Under the conditions, intermicellar thermodynamic and hydrodynamic interactions more or less affect solution properties of the micelles and are not easily separated in the evaluation of the micellar growth with concentration.

In the recent work, we have studied $C_{12}E_6$ and $C_{14}E_6$ micelles,[14] $C_{14}E_8$, $C_{16}E_8$, and $C_{18}E_8$ micelles,[15] $C_{10}E_5$ and $C_{10}E_6$ micelles,[16] $C_{12}E_5$, $C_{12}E_7$, and $C_{14}E_7$ micelles,[17] in dilute aqueous solutions by SLS and DLS measurements. In order to evaluate separately two concentration-dependent contribution of micellar growth and intermicellar interactions to the SLS results, we have utilized a thermodynamic theory[18,19] of light scattering for micellar solutions formulated with the wormlike spherocylinder model. The analyses have succsessfully yielded the values of the molar mass M_w of the micelles as a function of concentration c, along with values of the cross-sectional diameter d. It has been found that M_w increases as $M_w \propto c^{1/2}$ in agreement with the theoretical prediction derived on the basis of the association–dissociation equilibria for wormlike micelles.[18,20–22] The hydrodynamic radius R_H and mean-square radius of gyration $\langle S^2 \rangle$ as functions of M_w have been found to be well described by the corresponding theories[23–26] with wormlike spherocylinder or chain model, providing the information of the micellar characteristics such as d and flexibility.

In this work, we have studied the micelles of $C_{12}E_5$, $C_{12}E_6$, $C_{12}E_7$, and $C_{14}E_7$ by viscometry. Here, we have determined intrinsic viscosities of the micelles present at a specific concentration c, without resort to the extrapolation of the specific viscosity η_{sp} or the relative viscosity η_r to zero concentration as usually done in the studies of dilute polymer solutions.

EXPERIMENTAL SECTION

Materials

High-purity $C_{12}E_5$, $C_{12}E_6$, $C_{12}E_7$, and $C_{14}E_7$ samples were purchased from Nikko Chemicals Co. Ltd. and used without further purification. The solvent water used was high purity (ultrapure) water prepared with Simpli Lab water purification system of Millipore Co.

†To whom correspondence should be addressed (E-mail: einaga@cc.nara-wu.ac.jp).

Viscometry

Viscosity measurements were performed to obtain the intrinsic viscosity $[\eta]$ of the $C_{12}E_5$, $C_{12}E_6$, $C_{12}E_7$, and $C_{14}E_7$ micelles. We employed a four-bulb spiral capillary viscometer of the Ubbelohde type.[27,28] The four bulbs were used to vary the shear rate applied to the micelle solutions. The apparent shear rate G for the four bulbs and their combinations may be calculated according to the equation

$$G = \frac{h\rho g a}{2\eta_s \eta_r \ell} \tag{1}$$

Here, a and ℓ are the inner radius and length of the capillary, respectively, h is the height of the midpoint between the upper and lower marks for each bulb or a set of two or three bulbs above the exit of a liquid column from the capillary, ρ is the density of the liquid, g is the acceleration of gravity, and η_s is the solvent viscosity. The apparatus is designed to give small values of h so that the shear rate may be rather reduced.

In the studies of dilute polymer solutions, intrinsic viscosity $[\eta]$ is usually determined by the extrapolation to zero concentration by Huggins and Fuoss–Mead plots based on the equations

$$\eta_{sp}/c = [\eta] + k'[\eta]^2 c \tag{2}$$

$$\ln \eta_r/c = [\eta] - \beta[\eta]^2 c \tag{3}$$

where k' is the Huggins coefficient and β is related to k' by

$$k' + \beta = 1/2 \tag{4}$$

The usual procedure cannot be, however, applied to the micelle solutions, since the micellar size and hence $[\eta]$ of the micelles decreases with deceasing concentration c as mentioned in the Introduction. In the present study, we thus used the following equation to obtain $[\eta]$

$$[\eta] = \frac{[2(\eta_{sp} - \ln \eta_r)]^{1/2}}{c} \tag{5}$$

which is derived from eqs 2 and 3 with the relation (4). Here, the symbol $[\eta]_{app}$ is used to denote $[\eta]$ thus determined, since it is uncertain whether or not the concentration ranges of the present micelle solutions examined are dilute enough to warrant the validity of eqs 2 and 3. $[\eta]_{app}$ was obtained at various concentrations in the range of temperature T from 20.0 to 30.0 °C for the $C_{12}E_5$ micelles, from 25.0 to 45.0 °C for the $C_{12}E_6$ micelles, from 45.0 to 60.0 °C for the $C_{12}E_7$ micelles, from 30.0 to 55.0 °C for the $C_{14}E_7$ micelles.

The micellar solutions were prepared by dissolving appropriate amount of the surfactant in water. Complete mixing and micelle formation were achieved by stirring using a magnetic stirrer at least for one day. The weight concentrations w of test solutions were determined gravimetrically and converted to mass concentrations c by the use of the densities ρ of the solutions given previously.[14,17]

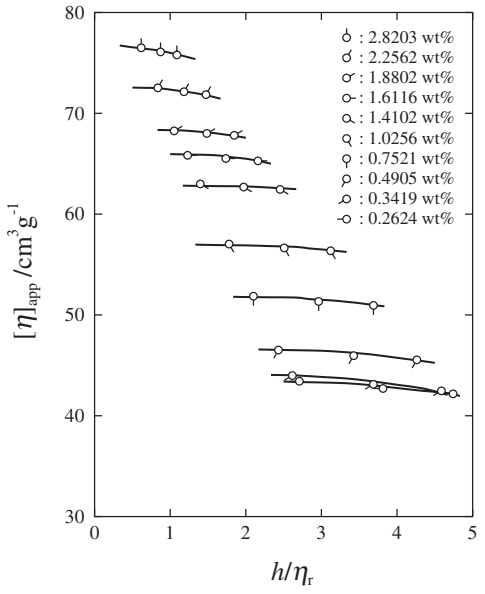

Figure 1. Shear rate dependence of the apparent intrinsic viscosity $[\eta]_{app}$ for the $C_{12}E_5$ micelles at various concentrations indicated at 20.0 °C.

RESULTS AND DISCUSSION

Shear Rate Dependence of the Apparent Intrinsic Viscosity

Figures 1, 2, and 3 depict examples of shear rate dependence of the apparent intrinsic viscosity $[\eta]_{app}$ for the $C_{12}E_5$ micelles at various concentrations indicated at 20.0, 25.0, and 30.0 °C, respectively. Here, $[\eta]_{app}$ is plotted against h/η_r which is proportional to the shear rate G as can be found in eq 1. The $[\eta]_{app}$ value at fixed concentration and temperature slightly decreases with increasing h/η_r, showing the non-Newtonian behavior. We can see that the magnitude of the decrease becomes slightly more significant for the micelles at higher concentrations and temperatures. The results for other micelles examined in the present study showed the similar behavior to those in these figures. According to these results, we have employed the value of $[\eta]_{app}$ at the lowest h/η_r at each fixed temperature and concentration as the zero-shear-rate value of $[\eta]_{app}$.

Concentration Dependence of the Apparent Intrinsic Viscosity

All of the values of $[\eta]_{app}$ at zero shear rate for the $C_{12}E_5$, $C_{12}E_6$, $C_{12}E_7$, and $C_{14}E_7$ micelles at various concentrations and temperatures are summarized in

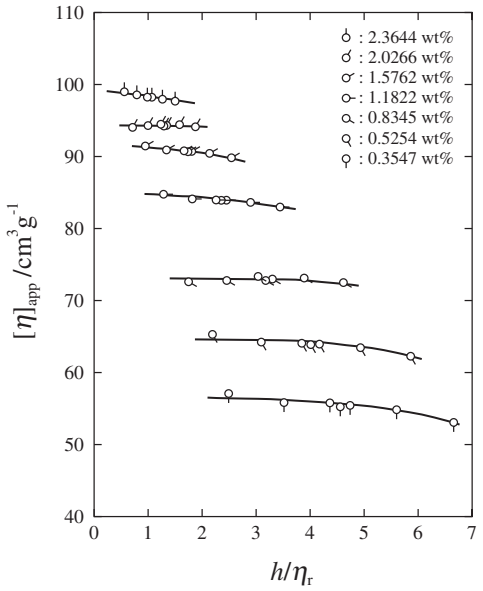

Figure 2. Shear rate dependence of the apparent intrinsic viscosity $[\eta]_{app}$ for the $C_{12}E_5$ micelles at various concentrations indicated at 25.0 °C.

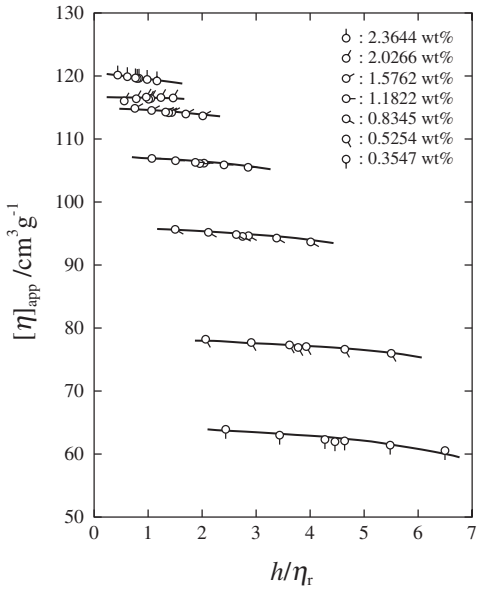

Figure 3. Shear rate dependence of the apparent intrinsic viscosity $[\eta]_{app}$ for the $C_{12}E_5$ micelles at various concentrations indicated at 30.0 °C.

Tables I, II, III, and IV, respectively, along with those of the molar mass M_w. Here, the results of M_w are reproduced from the previous papers,[14,17] for convenience. As mentioned in the Introduction, the M_w values for the respective micelles at a specific concentration were determined by the analyses of the SLS data with the aid of a thermodynamic theory[18] of SLS for micelle solutions.

In Figures 4, 5, 6, and 7, $[\eta]_{app}$ is plotted against c for the $C_{12}E_5$, $C_{12}E_6$, $C_{12}E_7$, and $C_{14}E_7$ micelles at various temperatures, respectively. For any micelle,

Table I. Values of M_w and $[\eta]_{app}$ for $C_{12}E_5$ micelles at various T and c

$10^2 c$/g cm^{-3}	$10^{-4} M_w$*	$[\eta]_{app}$/cm^3 g^{-1}
	$T = 20.0$ °C	
0.2619	68.3	43.4
0.3412	78.0	44.0
0.4896	93.4	46.5
0.7507	116	51.9
1.0237	135	57.0
1.4076	159	63.0
1.6087	170	65.8
1.8768	183	68.3
2.2522	201	72.5
2.8152	225	76.5
	$T = 25.0$ °C	
0.3536	145	57.1
0.5239	176	65.3
0.8320	222	72.6
1.1787	264	84.8
1.5716	305	91.5
2.0206	346	94.1
2.3574	374	99.0
	$T = 30.0$ °C	
0.3531	227	63.9
0.5231	276	78.2
0.8308	348	95.7
1.1770	414	107
1.5694	478	115
2.0178	542	116
2.3541	585	120

*Results by Shirai and Einaga.[17]

$[\eta]_{app}$ at fixed temperature increases with c following a curve convex upward. It also increases with raising temperature. The results are considered to come mainly from the fact that the C_iE_j micelles grow in size with increasing concentration and with raising temperature.[14–17] The increase in $[\eta]_{app}$ with c may, however, possibly reflect the enhancement of the intermicellar hydrodynamic interactions with concentration in addition to the effect of the micellar growth.

Molar Mass Dependence of the Intrinsic Viscosity

In order to examine properties of the micelles, we have double-logarithmically plotted $[\eta]_{app}$ against M_w in Figures 8 and 9, in which effects of the hydrophilic and hydrophobic chain lengths on the molar mass dependence of $[\eta]_{app}$ are shown, respectively. It is seen that the data points for each micelle at various T and c form a single composite curve, implying that the effects of the intermicellar hydrodynamic interactions on $[\eta]_{app}$ are negligible in the range of c studied. We may interpret the results as indicating that the present $[\eta]_{app}$, though determined at finite concentrations, correspond to $[\eta]$ for the "isolated" micelles formed at given concentrations. Here, we thus analyze

Table II. Values of M_w and $[\eta]_{app}$ for $C_{12}E_6$ micelles at various T and c

$10^2 c/g\,cm^{-3}$	$10^{-4}M_w$*	$[\eta]_{app}/cm^3\,g^{-1}$
	$T = 25.0\,^\circ C$	
0.6984	11.4	4.04
1.0144	13.8	5.14
1.9022	18.9	7.55
2.2909	20.7	8.66
3.1275	24.3	10.3
4.1095	27.9	12.1
6.0147	33.9	15.3
	$T = 30.0\,^\circ C$	
1.0676	23.3	9.26
1.4853	27.4	11.6
2.0576	32.3	14.0
2.4933	35.6	15.6
2.9015	38.4	16.9
3.9185	44.7	19.8
	$T = 35.0\,^\circ C$	
0.8165	352	14.9
1.4345	467	19.8
2.0344	556	23.3
2.7111	643	26.5
	$T = 40.0\,^\circ C$	
0.3159	34.3	13.3
0.5230	44.2	18.5
0.7289	52.2	22.0
1.0142	61.5	25.4
1.7574	81.1	32.6
	$T = 45.0\,^\circ C$	
0.3060	55.7	20.0
0.5174	72.4	24.1
0.7312	86.1	32.0
0.8078	90.5	33.0
1.0191	102	36.1
1.5095	124	41.8
2.0079	143	45.8
2.5066	160	48.6

*Results by Yoshimura *et al.*[14]

Table III. Values of M_w and $[\eta]_{app}$ for $C_{12}E_7$ micelles at various T and c

$10^2 c/g\,cm^{-3}$	$10^{-4}M_w$*	$[\eta]_{app}/cm^3\,g^{-1}$
	$T = 45.0\,^\circ C$	
1.7537	21.3	11.7
2.3383	24.6	12.2
2.8060	27.0	12.8
3.3889	29.7	13.8
4.2361	33.3	14.8
5.6482	38.7	16.4
6.7778	42.5	17.6
	$T = 50.0\,^\circ C$	
2.1134	42.6	15.7
3.0741	51.5	18.7
4.2269	60.5	20.6
5.6358	70.2	22.5
6.7630	77.1	23.7
	$T = 55.0\,^\circ C$	
2.1084	66.6	21.9
3.0668	80.4	25.5
4.2168	94.5	27.4
5.6224	109	28.6
6.7469	120	29.3
	$T = 60.0\,^\circ C$	
1.7413	90.0	28.7
2.3217	104	30.3
2.7861	114	31.3
3.3649	125	33.1
4.2062	140	33.9
5.6082	162	34.5
6.7299	178	34.4

*Results by Shirai and Einaga.[17]

the data by using the hydrodynamic theory for wormlike polymers.

The intrinsic viscosity $[\eta]$ for wormlike polymers is formulated by Yoshizaki *et al.*[29] with the wormlike touched-bead model. The expression for $[\eta]$ has been given as a function of the contour length L or number of beads N, bead diameter d_b, and stiffness parameter λ^{-1} over the entire range of L including the sphere, *i.e.*, the case $L = d_b$. It reads

$$[\eta] = \frac{6^{3/2}\Phi_\infty \langle S^2\rangle^{3/2}}{M} f_\eta(\lambda L, \lambda d_b) + [\eta]_E \qquad (6)$$

$$\lambda^2\langle S^2\rangle = \frac{\lambda L}{6} - \frac{1}{4} + \frac{1}{4\lambda L} - \frac{1}{8(\lambda L)^2}(1 - e^{-2\lambda L}) \qquad (7)$$

$$[\eta]_E = \frac{5\pi N_A N d_b^3}{12M} \qquad (8)$$

where the Flory's viscosity coefficient $\Phi_\infty = 2.870 \times 10^{23}$, M is the molecular weight, N_A is the Avogadro's number, and $[\eta]_E$ denotes the intrinsic viscosity of the Einstein spheres. It is to be noted that $L = Nd_b$. It has been shown[29] that the values of $[\eta]$ calculated by eq 6 coincide with those calculated with the wormlike cylinder model in the range of large L, if the cross-sectional diameter d of the latter model is taken to be $0.74d_b$; the latter values are available only at large L. We may, thus, calculate $[\eta]$ for the wormlike spherocylinder model by using the relation $d_b = d/0.74$. The expression for the function f_η is so lengthy that we refer it to the original paper.[29]

For the micelles, the values of weight-average contour length L_w may be calculated by

$$L_w = \frac{4\nu M_w}{\pi N_A d^2} + \frac{d}{3} \qquad (9)$$

where ν is the partial specific volume of the micelle. By eqs 6–8, we may calculate $[\eta]$ as a function of M_w by using L_w by eq 9 in place of L and M_w in place of M in these equations and by assigning proper values of the parameters d and λ^{-1}. In this work,

Table IV. Values of M_w and $[\eta]_{app}$ for $C_{14}E_7$ micelles at various T and c

$10^2 c$/g cm^{-3}	$10^{-4} M_w$*	$[\eta]_{app}$/cm^3 g^{-1}
	$T = 30.0\,^\circ$C	
1.0261	20.4	12.8
1.5784	25.3	13.2
2.0518	28.8	13.7
2.9306	34.5	15.9
4.1019	40.9	18.9
4.1376	41.1	20.0
4.9644	45.0	21.5
	$T = 35.0\,^\circ$C	
1.0790	59.7	22.3
1.9779	80.9	27.2
2.9663	99.3	32.2
3.3898	106	34.5
	$T = 40.0\,^\circ$C	
1.0770	44.7	133
1.9741	54.6	180
2.9606	62.6	221
3.9467	69.7	256
4.7354	72.2	280
	$T = 50.0\,^\circ$C	
4.7171	833	106
	$T = 55.0\,^\circ$C	
0.4517	366	89.7
0.6775	448	99.5
1.0162	549	111

*Results by Shirai and Einaga.[17]

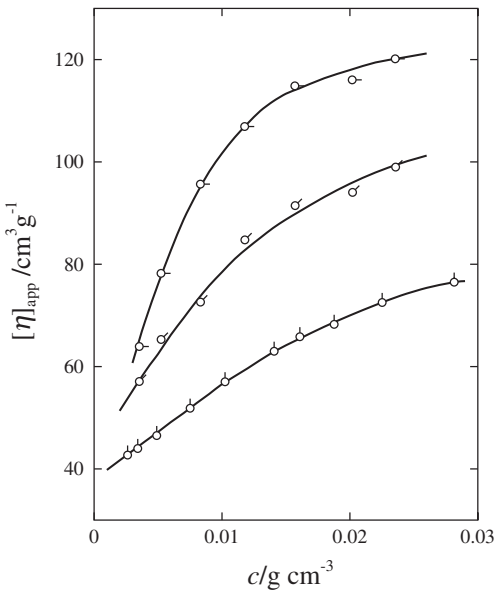

Figure 4. Concentration dependence of the apparent intrinsic viscosity $[\eta]_{app}$ for the $C_{12}E_5$ micelles at various temperatures: Pips with directions of succesive 45° clockwise rotations from pip up correspond to 20.0, 25.0, and 30.0 °C, respectively.

the theoretical values of $[\eta]$ have been calculated as a function of M_w for various values of d with the use of the λ^{-1} values determined previously[14,17] for the

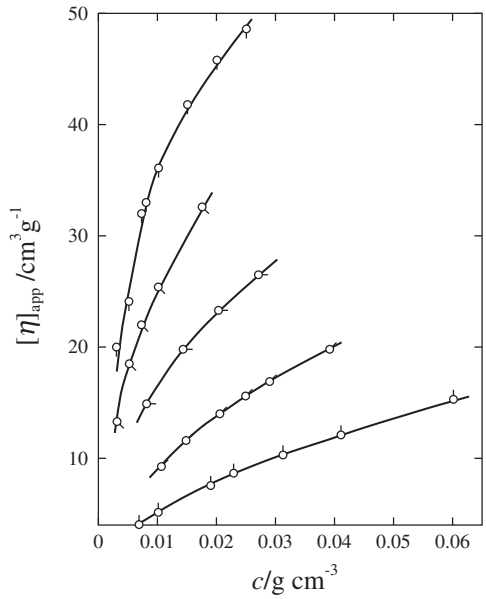

Figure 5. Concentration dependence of the apparent intrinsic viscosity $[\eta]_{app}$ for the $C_{12}E_6$ micelles at various temperatures: Pips with directions of succesive 45° clockwise rotations from pip up correspond to 25.0, 30.0, 35.0, 40.0, and 45.0 °C, respectively.

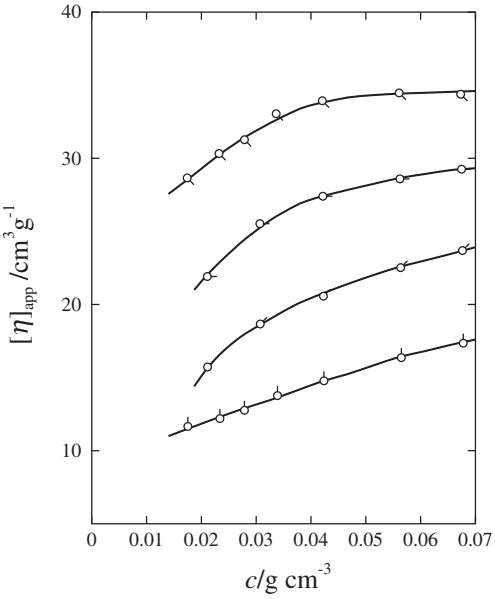

Figure 6. Concentration dependence of the apparent intrinsic viscosity $[\eta]_{app}$ for the $C_{12}E_7$ micelles at various temperatures: Pips with directions of succesive 45° clockwise rotations from pip up correspond to 45.0, 50.0, 55.0, and 60.0 °C, respectively.

$C_{12}E_5$, $C_{12}E_6$, $C_{12}E_7$, and $C_{14}E_7$ micelles from the analyses of the hydrodynamic radius R_H as a function of M_w with the wormlike spherocylinder model. In Figures 8 and 9, the solid lines are best-fit curves to the data points for the corresponding micelles. It is found that the theoretical curves well describe the observed behavior of $[\eta]$, although the data points for the $C_{12}E_6$ micelles decreases rather steeply with

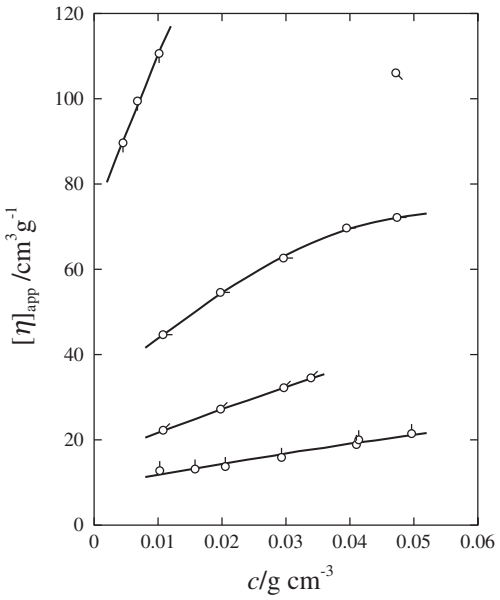

Figure 7. Concentration dependence of the apparent intrinsic viscosity $[\eta]_{app}$ for the $C_{14}E_7$ micelles at various temperatures: Pips with directions of succesive 45° clockwise rotations from pip up correspond to 30.0, 35.0, 40.0, 50.0, and 55.0 °C, respectively.

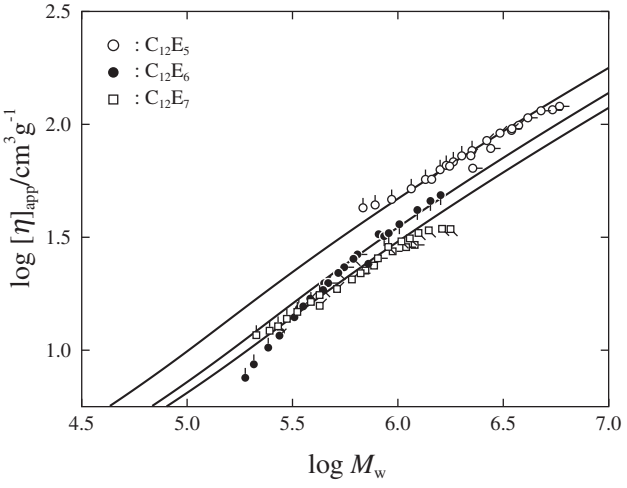

Figure 8. Molecular weight dependence of the apparent intrinsic viscosity $[\eta]_{app}$ for the $C_{12}E_5$, $C_{12}E_6$, and $C_{12}E_7$ micelles. The directions of the pips have the same meaning as those in Figures 4, 5, and 6. The solid curves represent the theoretical values calculated by eqs 6–9.

Table V. Values of λ^{-1} and d for $C_{12}E_5$, $C_{12}E_6$, $C_{12}E_7$, and $C_{14}E_7$ micelles

	λ^{-1}/nm (R_H)*	d/nm ([η])	d/nm (SLS)*
$C_{12}E_5$	12	2.4	2.2
$C_{12}E_6$	14	2.8	2.3
$C_{12}E_7$	14	3.0	2.4
$C_{14}E_7$	13	2.7	2.4

*Results by Yoshimura *et al.*[14] and by Shirai and Einaga.[17]

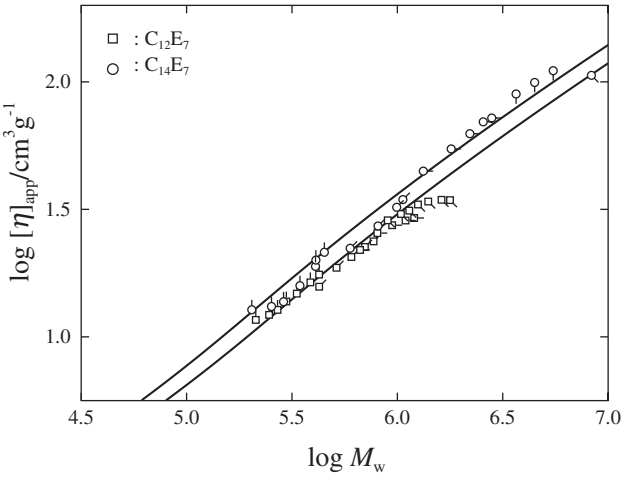

Figure 9. Molecular weight dependence of the apparent intrinsic viscosity $[\eta]_{app}$ for the $C_{12}E_7$ and $C_{14}E_7$ micelles. The directions of the pips have the same meaning as those in Figures 6 and 7. The solid curves represent the theoretical values calculated by eqs 6–9.

decreasing M_w in the range of small M_w for the reason unknown at present. The good agreement between the theoretical and observed results implies that the micelles assume a flexible cylindrical shape which may be represented by the wormlike spherocylinder model. These results are in accordance with the previous findings[14,17] from the c dependence of the SLS data and M_w dependence of R_H and $\langle S^2 \rangle$.

Cross-sectional Diameter of the Micelles

The values of d obtained by the curve fittings are listed in Table V along with those of λ^{-1} used. The table also includes the d values determined previously[14,17] from the analyses of the SLS results for comparison. The results indicate that d increases with the hydrophilic chain length j when the hydrophobic chain length i is fixed. On the other hand, d decreases or remains unchanged with increasing i at fixed j.

The present d values obtained from $[\eta]$ are somewhat larger than those from the SLS results. We note that the d values from SLS quantitatively explain M_w dependence of the hydrodynamic radius R_H at sufficiently low concentrations in combination with the results of λ^{-1} given in Table V;[14,17] in actuality, the λ^{-1} values have been obtained from the analyses of the R_H *vs.* M_w data by using the d values from the SLS results. This means that the same set of the values of d and λ^{-1} cannot concurrently describe both $[\eta]$ and R_H as functions of M_w. The differences may be attributed to the fact that there is a distribution in micellar size and different averages are reflected in the $[\eta]$, R_H, and SLS data. In this connection, it is to be noted that as shown in the previous studies,[14,17] the micelles observed in this study have the most probable

distribution in size which affords a value 2 as the ratio of the weight-average aggregation number N_w to the number-average N_n irrespective of T and c.

The results of d provide us with information about conformation of the surfactant molecules in the micelles. According to the Flory's RIS (rotational isomeric state) calculations,[30] the root-mean-square end-to-end distances $\langle R^2 \rangle^{1/2}$ of n-dodecane and n-tetradecane are 1.01 and 1.15 nm, respectively. The RIS calculations give 1.00, 1.12, and 1.22 nm for $\langle R^2 \rangle^{1/2}$ of penta-, hexa, and hepta-oxyethylene chains, respectively. From these $\langle R^2 \rangle^{1/2}$ values, we obtain 3.01, 3.25, 3.45, and 3.59 nm for the d values of the $C_{12}E_5$, $C_{12}E_6$, $C_{12}E_7$, and $C_{14}E_7$ micelles, provided that the alkyl groups of the surfactant molecules exist in the hydrophobic core in a similar state to the bulk state of amorphous polyethylene and that the oxyethylene groups are oriented straightforwardly in the radial direction. These calculated values are roughly comparable to the observed ones, indicating that the alkyl and oxyethylene chains of the surfactant molecules do not take the fully extended form but the randomly coiled form in the micelles. The differences between the calculated and observed values of d may suggest that the oxyethylene chains are moving by taking a random orientation in water.

CONCLUSIONS

In the present work, we have characterized the $C_{12}E_5$, $C_{12}E_6$, $C_{12}E_7$, and $C_{14}E_7$ micelles by viscometry. It has been demonstrated that the intrinsic viscosity $[\eta]$ of the micelles whose size is concentration-dependent can be determined at a specific concentration by utilizing an equation derived with a combination of the Huggins and Fuoss–Mead equations. The present method may also be applicable to solutions of the polymer aggregates whose size varies with polymer concentration.

The results of $[\eta]$ have been analyzed with the hydrodynamic theory[29] for wormlike polymers formulated with the touched-bead model. The good agreement between the calculated and observed $[\eta]$ as a function of the molar mass M_w indicates that the present micelles assume a shape of wormlike spherocylinders in dilute solutions. The analyses have yielded the cross-sectional diameter d which increases with increasing hydrophilic chain length at fixed length of the hydrophobic chain. The d values have suggested that the alkyl and oxyethylene groups of the surfactant molecules do not assume the fully extended form but are randomly coiled.

Acknowledgment. The authors are grateful to Prof. Takenao Yoshizaki at Kyoto University and also to members of the NKO Academy for valuable discussions and comments. This research was supported in part by Nara Women's University Intramural Grant for Project Research.

REFERENCES

1. A. Bernheim-Groswasser, E. Wachtel, and Y. Talmon, *Langmuir*, **16**, 4131 (2000).
2. W. Brown, R. Johnson, P. Stilbs, and B. Lindman, *J. Phys. Chem.*, **87**, 4548 (1983).
3. T. Kato and T. Seimiya, *J. Phys. Chem.*, **90**, 1986 (1986).
4. W. Brown and R. Rymden, *J. Phys. Chem.*, **91**, 3565 (1987).
5. W. Brown, Z. Pu, and R. Rymden, *J. Phys. Chem.*, **92**, 6086 (1988).
6. T. Imae, *J. Phys. Chem.*, **92**, 5721 (1988).
7. W. Richtering, W. Burchard, and H. Finkelmann, *J. Phys. Chem.*, **92**, 6032 (1988).
8. T. Kato, S. Anzai, and T. Seimiya, *J. Phys. Chem.*, **94**, 7255 (1990).
9. H. Strunk, P. Lang, and G. H. Findenegg, *J. Phys. Chem.*, **98**, 11557 (1994).
10. P. Schurtenberger, C. Cavaco, F. Tiberg, and O. Regev, *Langmuir*, **12**, 2894 (1996).
11. G. Jerke, J. S. Pedersen, S. U. Egelhaaf, and P. Schurtenberger, *Langmuir*, **14**, 6013 (1998).
12. O. Glatter, G. Fritz, H. Lindner, J. Brunner-Papela, R. Mittelbach, R. Strey, and S. U. Egelhaaf, *Langmuir*, **16**, 8692 (2000).
13. T. R. Carale and D. Blankschtein, *J. Phys. Chem.*, **96**, 455 (1992).
14. S. Yoshimura, S. Shirai, and Y. Einaga, *J. Phys. Chem. B*, **108**, 15477 (2004).
15. N. Hamada and Y. Einaga, *J. Phys. Chem. B*, **109**, 6990 (2005).
16. K. Imanishi and Y. Einaga, *J. Phys. Chem. B*, **109**, 7574 (2005).
17. S. Shirai and Y. Einaga, *Polym. J.*, in press.
18. T. Sato, *Langmuir*, **20**, 1095 (2004).
19. R. Koyama and T. Sato, *Macromolecules*, **35**, 2235 (2002).
20. D. Blankschtein, G. M. Thurston, and G. B. Benedek, *J. Chem. Phys.*, **85**, 7268 (1986).
21. M. E. Cates and S. J. Candou, *J. Phys.: Condens. Matter*, **2**, 6869 (1990).
22. N. Zoeller, L. Lue, and D. Blankschtein, *Langmuir*, **13**, 5258 (1997).
23. T. Norisuye, M. Motowoka, and H. Fujita, *Macromolecules*, **12**, 320 (1979).
24. H. Yamakawa and M. Fujii, *Macromolecules*, **6**, 407 (1973).
25. H. Yamakawa and T. Yoshizaki, *Macromolecules*, **12**, 32 (1979).
26. H. Benoit and P. Doty, *J. Phys. Chem.*, **57**, 958 (1953).
27. J. H. Larkins, J. D. Perrings, G. R. Shepherd, and B. J. Noland, *J. Chem. Educ.*, **42**, 555 (1965).
28. Y. Miyaki, Ph. D. Thesis, Osaka University, 1981.
29. T. Yoshizaki, I. Nitta, and H. Yamakawa, *Macromolecules*, **21**, 165 (1988).
30. P. J. Flory, "Statistical Mechanics of Chain Molecules," John Wiley & Sons, New York, 1969.